Available online at www.sciencedirect.com
ScienceDirect
Journal of the European Ceramic Society 26 (2006) 3599–3606
www.elsevier.com/locate/jeurceramsoc

Agglomeration on drying of yttria-stabilised-zirconia slurry on a metal substrate

Weihua Lan, Xin Wang, Ping Xiao *

School of Materials, University of Manchester, Manchester M1 7HS, UK

Received 15 July 2005; received in revised form 2 December 2005; accepted 9 December 2005
Available online 23 February 2006

Abstract

Drying behaviour of aqueous yttria-stabilised-zirconia (YSZ) slurry on a metal substrate has been investigated by examining drying kinetics, shrinkage rate and cracking behaviour as a function of agglomeration degree. The agglomeration behaviour of the slurry was varied by changing its pH value, and evaluated by measuring both zeta-potential and viscosity. The drying kinetics of the slurries on substrates was characterized with weight loss and classified as an initial constant rate period (CRP) followed by a falling rate period (FRP). Uneven thickness reduction, measured using optical microscope, occurred in the CRP stage due to lateral flow, and became more uniform with increase in agglomeration degree. Tensile stresses developed within the coating because of the substrate constraint and resulted in crack formation and propagation. Cracking behaviour was controlled by the agglomeration degree of the slurry.

Keywords: Drying; ZrO_2; Slurry; Agglomeration

1. Introduction

Ceramic slurry or suspension is made with dispersion of ceramic particles in a liquid, and stabilized by the repulsive interaction between particles. In colloidal processing, stable slurry or suspension consolidates to form a densely packed structure, whereas unstable one may lead to a loosely packed structure.[1] In general, an aqueous suspension can be stabilized by one of two methods[2]: (1) adjusting pH value away from the particle's isoelectric point (IEP) to induce electrostatic repulsion; (2) adsorbing organic molecules to induce steric repulsion.

To remove the liquid before firing, drying is a critical step, during which cracking, fracture and delamination often occur. A classical work on the study of the drying kinetics of gel[3] shows that the drying of porous bulk material is generally composed of three stages, i.e. an initial constant rate period (CRP) followed by two falling rate periods (FRPI and FRPII). In the CRP stage, liquid is transported to the exterior surface by capillary force, where evaporation occurs, and the wet particulate body shrinks continuously under compression.[3] The extent of shrinkage is governed by the balance between the capillary force exerted by the pore liquid and the strength of the solid network which resists shrinkage.[4]

Colloidal processing techniques, including slurry coating, dip coating, spin coating or electrophoretic deposition (EPD), have been used to produce thin films and coatings in the past decades. The wet coating, prepared by slurry coating technique[5] or EPD,[6] shrinks mostly along the thickness direction, and biaxial tensile stresses arise within the coating due to constraint in the *XY*-plane by the substrate. When the tensile stresses exceed the local tensile strength, cracks form and propagate, which is controlled by the microstructure of the coating and the strength of the inter-particle bond.[7]. Chiu et al.[8,9] found that granular ceramic films cracked during drying when they were prepared with a thickness greater than the critical cracking thickness (CCT). They pointed out that ceramic particle size, liquid surface tension and suspension stability had the most pronounced influence on the CCT of the film. Recently, Guo and Lewis[10] investigated the influence of agglomeration phenomena on the drying behaviour of colloidal silica films, and showed that the inter-particle forces played a decisive role in the film formation process. The solid network strength increased with increase in the agglomeration degree, accordingly, higher compressive force was required to consolidate the agglomerated suspensions. Finally, a densely packed

* Corresponding author. Tel.: +44 161 306 5941; fax: +44 161 306 3586.
E-mail address: ping.xiao@manchester.ac.uk (P. Xiao).

0955-2219/$ – see front matter © 2006 Elsevier Ltd. All rights reserved.
doi:10.1016/j.jeurceramsoc.2005.12.026

microstructure was obtained for the film prepared from a well dispersed suspension.

The dispersion state of particles in a suspension clearly has a strong influence on the drying behaviour and structure evolution of colloid coatings. Previous studies[8–10] mainly focused on the drying process of the coatings with a thickness less than CCT, which did not crack during drying, and overlooked the effect of dispersion state on crack development and shrinkage behaviour. In fact, cracking is always a big problem for the slurry coating process, and different shrinkage-crack patterns have been observed in previous studies.[11,12] Knowledge of cracking and fragmentation phenomenon is of increasing interest in controlling the colloidal process to fabricate coatings on substrates.

A previous work[13] has studied drying of aqueous YSZ slurries on metal substrates with different initial water contents, and found that drying started with an initial CRP, followed by FRP. Thickness reduction mostly occurred during CRP, and lateral flow led to uneven thickness of the dried coating. Cracking mostly occurred in the FRP stage due to the substrate constraint on the top coating. In this work, the study has been focused on the effect of slurry agglomeration on drying behaviour. The agglomeration degree of the slurry was varied by changing its pH value. The influence of the agglomeration phenomena on the drying behaviour of the YSZ slurry was investigated by in situ measuring weight loss, thickness reduction and monitoring crack development. The relations between agglomeration degree, shrinkage behaviour and crack formation have been discussed.

2. Experimental procedure

2.1. Materials

Aqueous slurry of yttria-stabilised-zirconia (XZO1357/01, MEL Chemicals, UK) was used as starting material, which is with composition of 8 wt.% Y_2O_3–ZrO_2, solid content of 18 wt.% and primary particle size of 12 nm. The pH value of the as-received slurry was adjusted to be 3, 4.5, 5.5 and 7.5, respectively, by the addition of dilute hydrochloric acid (HCl) with continuous magnetic stirring. After 24 h stirring, the slurries with different pH values were concentrated to a high solid content of 47–50 wt.% by drying at room temperature. The agglomeration degree of the slurry was evaluated by measuring the zeta-potential and viscosity of the as-received slurry with 18 wt.% solid content. The zeta-potential was measured as a function of pH value using a zeta-potential analyzer (Delsa 440SX). The viscosity was measured at shear rates from 5 to 100 s^{-1} using a cone-plate viscometer (BROOKFIELD, VIII-Rhometer).

2.2. Drying experiments

Drying experiments were carried out on the pre-concentrated slurries with 47–50 wt.% solid content. A circular mould was made of aluminum metal, where a 500 μm depth and 10 mm diameter hole was drilled. The contact angle of water on the aluminum metal was measured to be $78 \pm 3^\circ$. The mould was glued to a Fecralloy substrate (1 mm thick, Fe72.8/Cr22/Al5/Y0.1/Zr0.1, Goodfellow, UK), which had been polished using SiO_2 sand paper (P600, HERMES) and cleaned in an ultrasonic bath. The slurry was cast into the mould and smoothed using a blade to form wet coatings with a thickness of 500 μm and a diameter of ϕ 10 mm. After casting, the mould was enclosed in a sample holder with two sleeves. The inner diameter of the inner sleeve had the same dimensions as the coating, so that the effect of convection was reduced. The sample holder was placed on a weight balance (Ohaus AB-S) with a sensitivity of 0.01 mg. The weight of the wet coating was recorded every minute, using a PC equipped with TAL Technologies Win Wedge software. Drying rates were calculated as weight loss/min. For each experiment, at least three samples were repeated, and the results were reproducible.

The thickness reduction of the wet coating was measured separately, using a calibrated optical microscope (Olympus). The thickness reduction was recorded every 3 min by measuring the focused position using a magnification of 200. In this work, two focused positions were selected, i.e. one was at the coating edge, while the other was at the coating centre. The thickness shrinkage was calculated as the decrease of the thickness over the initial thickness of the coating.

Images of the coating surface were in situ taken using a video camera. Fig. 1 sketches a schematic image of the coating surface, which resembles a patchwork of polygonal fragments separated by cracks. The optical images were subjected to image analysis (UTHSCSA Image Tool). The area of the mould, A_{coat}, representing the initial area of the wet coating, and the areas of the fragments, A_i, were measured. The surface shrinkage, $S\%$, was calculated using Eq. (1):

$$S\% = \frac{A_{coat} - \sum_i A_i}{A_{coat}} \times 100\% \quad (1)$$

All drying experiments were carried out in an ambient environment. The temperature was 24.5–25 °C, and the relative humidity was 40–45%. The top surfaces of the dried fragments were examined using scanning electron microscope (FED-SEM, Philip XL 30).

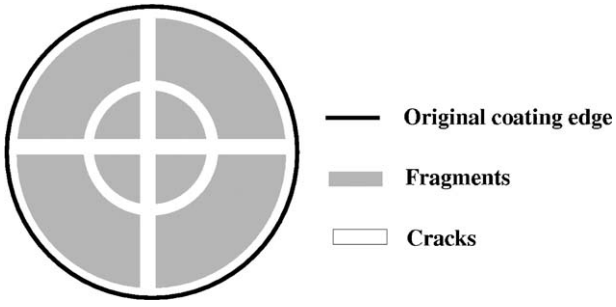

Fig. 1. Schematic of typical top surface morphology of a coating.

3. Results

3.1. Slurry characterization

Fig. 2 shows the zeta-potential of YSZ particles as a function of pH value. The isoelectric point (IEP) is determined as 8. With increase of the pH value from 3 to 7.5, the zeta-potential decreases. Fig. 3 shows the viscosity versus shear rate for the slurries with 18 wt.% solid content and different pH values (3, 5.5, 7.5). The slurry with pH 7.5 displays strong shear thinning behaviour and high viscosity, indicating a high agglomeration degree.[14] This is attributed to the comparatively lower zeta-potential at a pH value close to the IEP. The repulsive forces between particles are not big enough to shield the attractive van der Waals force, therefore, the particles form an attractive network. With decrease in the pH value, the degree of shear thinning decreases significantly. The slurry with pH 3 shows the lowest viscosity which is relatively independent of shear rate, suggesting that the particles are strongly repulsive and well dispersed. Compared with the slurries with pH 3 or 7.5, the slurry with pH 5.5 shows a medium viscosity, in which particles are weakly attractive.

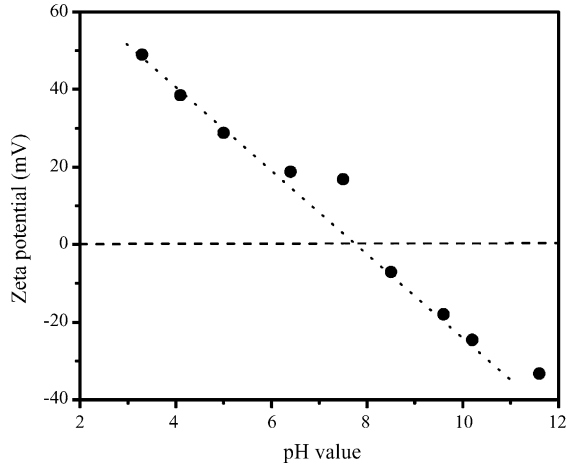

Fig. 2. Zeta-potential of YSZ particles as a function of pH value.

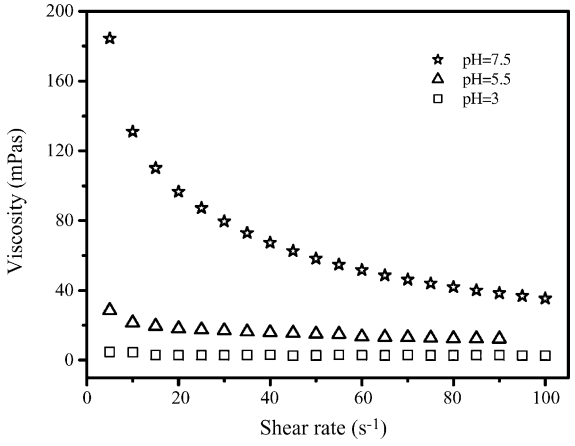

Fig. 3. Viscosity vs. shear rate for the slurries with 18 wt.% solid content.

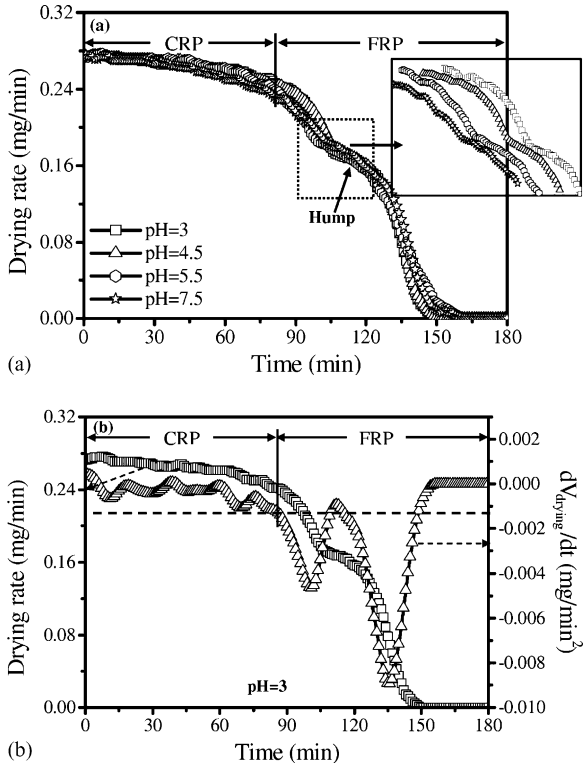

Fig. 4. (a) Drying rates as a function of drying time for the slurries with 47–50 wt.% solid content. Two-stage drying process, i.e. CRP and FRP, is labeled. (b) Both the drying rate and the differentiation curve (dV_{drying}/dt) as a function of drying time for the slurry with pH 3. The end point of CRP is defined as where the absolute value of the differentiation is larger than 0.0012 mg/min^2.

3.2. Drying kinetics

Fig. 4a shows the drying rates as a function of drying time for the slurries with 47–50 wt.% solid content. Irrespective of the pH value, the slurries show a similar drying process, which can be roughly divided into two stages, i.e. an initial constant rate period (CRP) followed by a falling rate period (FRP). The separation point between the CRP and FRP is obtained according to the differentiation curve (dV_{drying}/dt) of the drying rate plot,[13] as shown in Fig. 4b. The end point of CRP is defined as where the drying rate dramatically decreases and the absolute value of the differentiation is larger than 0.0012 mg/min^2, i.e. lower than the broken line in Fig. 4b. In the CRP stage, the drying rates of the slurries are almost constant and decrease slightly with time. In the FRP stage, the drying rate decreases considerably, and a 'hump' appears, where the decreasing trend of the drying rate reduces. With increase in the pH value, i.e. increase in the agglomeration degree, the 'hump' becomes less apparent, as shown by the magnified plots in Fig. 4a. In the drying of bulk materials,[15,16] they show no presence of the 'hump'.

3.3. Structure evolution

As water evaporated, the thickness of the coating decreased and cracks formed due to the constraint from substrate. Fig. 5 shows the drying rate and the thickness shrinkage against drying time, coupled with the optical images of the coating surface

which correspond to specific thickness shrinkage labeled by numbers. The thickness reduction, occurring in the CRP stage, is uneven along the coating surface and experiences three-rate shrinkage at the coating centre, and two-rate shrinkage at the coating edge. The shrinkage rate at the coating centre is low at the beginning, and increases afterwards, then decreases again until the shrinkage stops. The shrinkage at the coating edge starts at a high rate, followed by a lower rate. For the dispersed slurry with pH 3, the difference between the shrinkage rates at the centre and the edge is apparent, as shown in Fig. 5a, in which higher final thickness shrinkage is obtained at the coating centre compared to the coating edge. For the weakly agglomerated slurry with pH 5.5, the difference of the shrinkage between the coating edge and the coating centre becomes smaller (Fig. 5b), while, for the strongly agglomerated slurry with pH 7.5, the difference decreases further to become negligible (Fig. 5c).

As the drying proceeded, cracks started to form at the coating edge. For the coating cast from the dispersed slurry with pH 3, short cracks were first formed vertical to the coating periphery, later gradually propagated toward the coating centre in radial forms. The coating broke into many fragments which slightly contracted in the *XY*-plane with increase in the crack width. When the crack-pattern became stable without formation of new cracks and no crack widening, the dark fragments became brighter with the appearance of spiral and circular cracks, as shown in Fig. 5a (image 6 and 7), suggesting a symmetry-breaking fracture model.[12] For the coating cast from the strongly agglomerated slurry with pH 7.5, at the start of the drying, the coating contracted slowly in the *XY*-plane from the edge and an annular gap was formed between the coating edge and the mould wall, as shown in Fig. 5c (image 2). Later, the radial cracks originated from the coating edge and propagated toward the coating centre. For the coating cast from the weakly agglomerated slurry with pH 5.5, radial cracks were formed at the same time as the coating contraction occurred at the edge (Fig. 5b). It is noticed that the initial crack formation and propagation do not obviously affect the drying rate in the CRP stage, however, with the appearance of the spiral cracks and the finish of surface shrinkage, a 'hump' appears in the drying rate plot in the FRP stage, as shown in Fig. 5.

The surface shrinkage was obtained according to Eq. (1) by considering coating contraction at the edge and crack formation at the coating surface. Table 1 summarizes the shrinkage data in both the thickness direction and the *XY*-plane. Lagging of the surface shrinkage behind the thickness shrinkage was observed for the agglomerated slurry. With increase in the pH value, i.e. increase in the agglomeration degree, the final thickness shrinkage decreases with decrease in the difference between the coating edge and coating centre, whereas the surface shrinkage increases with increasing delay after the thickness shrinkage.

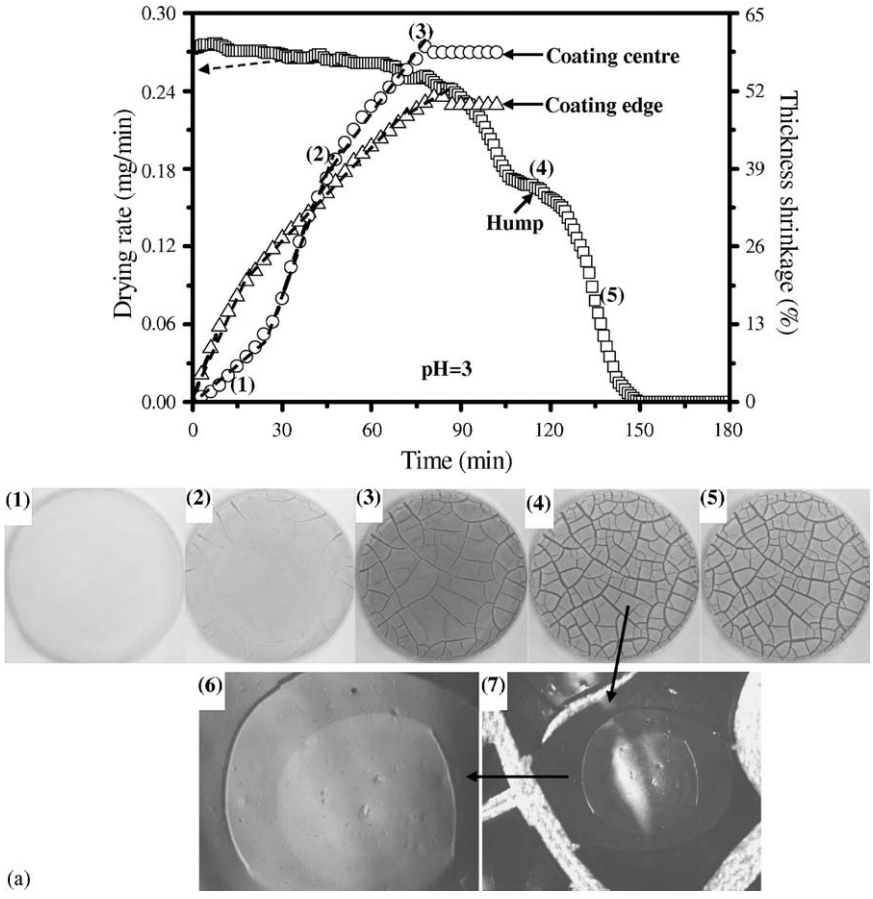

Fig. 5. Drying rate, thickness shrinkage and top surface image as a function of drying time for the slurries with 47–50 wt.% solid content and pH values at (a) pH 3; (b) pH 5.5; (c) pH 7.5. Optical images correspond to specific thickness shrinkage labeled by numbers.

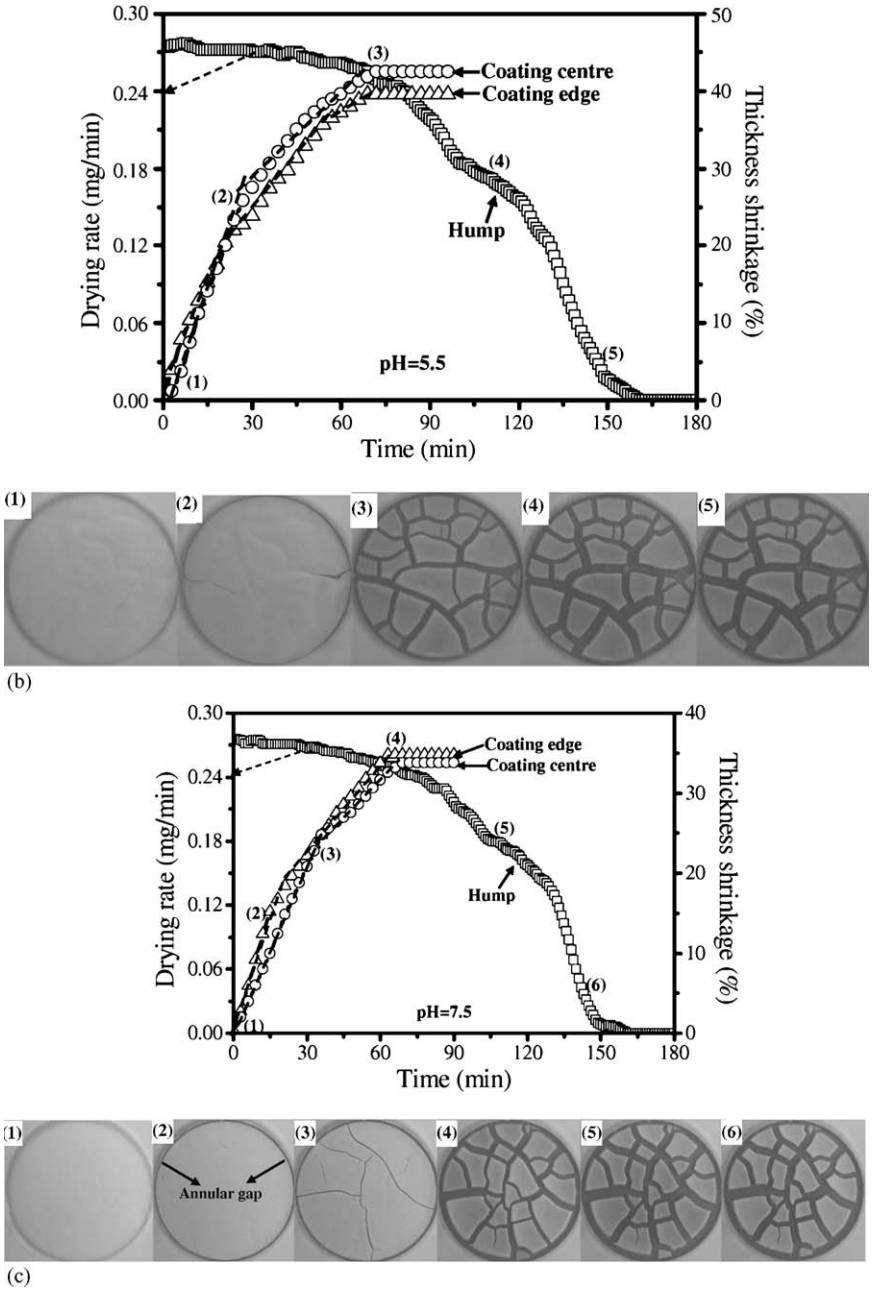

Fig. 5. (*Continued*).

Table 2 gives the time and residual water content when the first crack appeared in the coating, while the residual water content is obtained as the water weight in a wet coating over the weight of the coating. With increase in the pH value, the coating tends to crack earlier with higher residual water content. After the drying finishes, more fragments with narrower cracks are present in the coating with lower pH (Fig. 5).

Fig. 6 compares SEM micrographs of green compacts dried from the slurries with different pH values. The green compact dried from the dispersed slurry with pH 3 shows a dense

Table 1
Summary of shrinkage data

pH value of slurries	Final thickness shrinkage at the coating edge (%)	Final thickness shrinkage at the coating center (%)	Surface shrinkage when thick shrinkage stops (%)	Final surface shrinkage (%)
3	51	59	23	23
4.5	42	47	34	37
5.5	41	41	38	43
7.5	35	34	40	47

Table 2
Time and residual water contents (RWC) when cracks first form

Slurry	pH 3	pH 4.5	pH 5.5	pH 7.5
Time	45–54 min	33–42 min	15–24 min	6–15 min
RWC	(37.8 ± 1.8) wt.%	(42.9 ± 1.7) wt.%	(44.3 ± 1.3) wt.%	(49 ± 2.5) wt.%

microstructure, whereas the green compact dried from the strongly agglomerated slurry with pH 7.5 displays the least-dense microstructure, in which large pores are present. The green compacts dried from the weakly agglomerated slurries with pH 4.5, 5.5 show medium-dense microstructure.

4. Discussion

4.1. Drying kinetics

In the CRP stage, evaporation occurs at the top surface of the coating. Water is transported to the outside by capillary force, and the drying rate, V_{drying}, can be calculated as[3]:

$$V_{\text{drying}} = k\left[P_0 \exp\left(-\frac{V_{\text{m}}\gamma_{\text{LV}}\phi\rho_{\text{s}}S\cos\theta}{R_{\text{g}}T(1-\phi)}\right) - P_{\text{A}}\right] \quad (2)$$

where k is a constant and depends on the drying conditions, R_{g} is the ideal gas constant, T is the Kelvin temperature, P_0 is the vapor pressure of flat water, P_{A} is the ambient vapor pressure, V_{m} and γ_{LV} are the molar volume and the surface tension of water, and ϕ, S, ρ_{s} and θ are the volume fraction, specific surface area, theoretical density and water contact angle of solid particles, respectively.

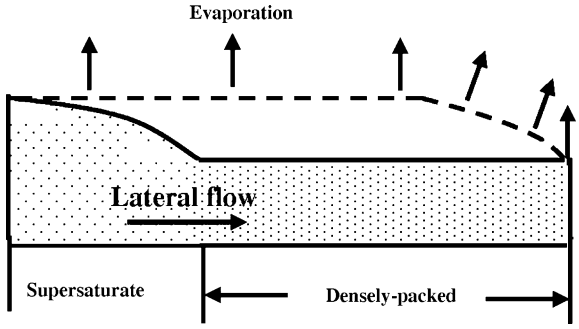

Fig. 7. Schematic of lateral drying in a wet coating cast with arc-edge.

Eq. (2) indicates that the drying rate of a wet coating is dependent on the solid volume fraction, i.e. the higher the solid volume fraction is, the lower the drying rate is. This is consistent with the experimental observation in Fig. 4a, the drying rates of the coatings decreases gradually in the CRP stage due to the increase in solid content in the wet coatings.

After the CRP, further evaporation drives the meniscus into the pores, and the drying rate is controlled by water transportation induced by capillary force.[3] Due to the increased distance between the top surface and drying front, the drying rate decreases considerably in the FRP stage. However, Fig. 4a shows that the decreasing trend of the drying rate reduces with the presence of a "hump" in the drying rate plot. It is believed that the release of tensile stresses due to coating delamination, which occurred with the appearance of spiral cracks, increases capillary force to transport water to coating surface, plus that increase in evaporation area due to exposure of the coating bottom surface with delamination also increases evaporation rate. Therefore, the decrease trend of drying rate reduces. Same

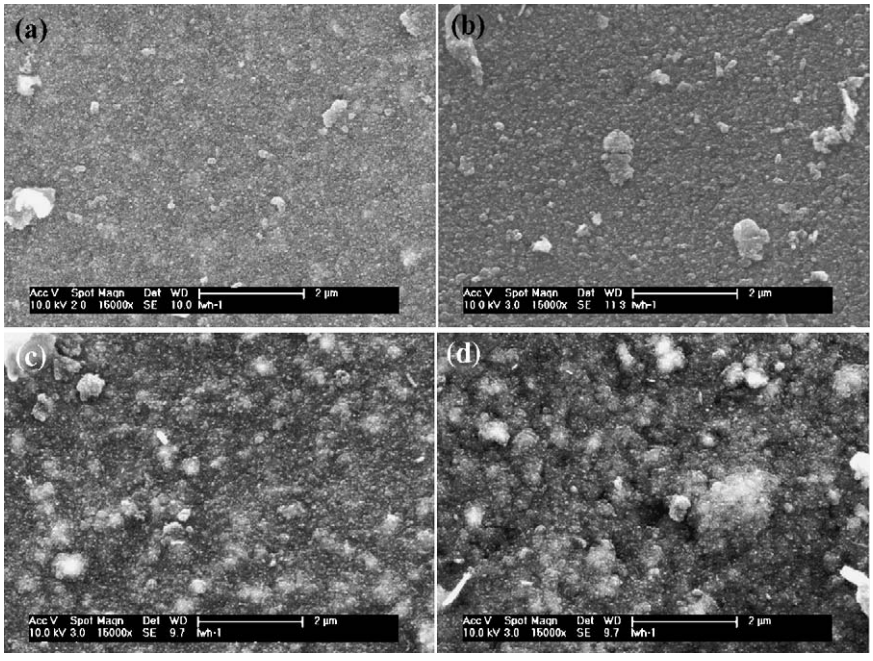

Fig. 6. SEM micrographs of green compacts dried from the slurries with 47–50 wt.% solid content and pH values at (a) pH 3; (b) pH 4.5; (c) pH 5.5; (d) pH 7.5.

phenomenon has been observed in a previous study,[13] which also showed a 'hump' in the drying rate plot in the FRP stage.

4.2. Shrinkage mechanism

The coating was observed to be cast in a shape as schematized in Fig. 7, which had higher vapor pressure at the arc-edge.[17,18] Therefore, higher evaporation rate was obtained at the coating edge, which induced higher thickness reduction rate at the coating edge than that at the coating centre, as measured in the early thickness reduction stage (Fig. 5). As the drying proceeded, particles first became densely packed at the coating edge due to higher evaporation rate, whereas, the coating centre was still in supersaturate state where particles were suspended in water and free to move (Fig. 7). Similar phenomena have been observed in other studies and termed as lateral drying.[13,19,20] In the densely packed region close to the coating edge, higher capillary force developed compared to that at the coating centre. A pressure gradient formed along the coating surface and drove water and free particles from the centre to the edge. Evaporated water from the coating edge could be partially replenished by the water and particles moved from the coating centre. Therefore, the thickness reduction rate at the coating edge decreased, while that at the coating centre increased due to losing water and particles to the coating edge, as measured in the later thickness reduction stage (Fig. 5). Because lateral flow moved free particles from the central region to the periphery, higher final thickness shrinkage was obtained at the coating centre than that at the coating edge for the coating cast from the dispersed slurry with pH 3 (Table 1). With increase in the pH value to 7.5, i.e. increase in the agglomerate degree, the slurry became more viscous (Fig. 3) with fewer free particles and were likely to cast with a flat surface with uniformed spatial pressure, and so lateral drying was not apparent and led to even thickness shrinkage of the coating (Fig. 5c).

Concurrently to the water evaporation and thickness reduction, tensile stresses developed in the coating due to the constrained volume shrinkage, and later were released by crack formation and propagation. According to the constitutive equations for a viscous gel,[21] the strain rate of a coating in the thickness direction, $\dot{\varepsilon}_z$, can be written as a function of the constrained stress, σ_{con}:

$$\dot{\varepsilon}_z = \dot{\varepsilon}_f - \frac{2N}{3F}\sigma_{con} \quad (3)$$

where $\dot{\varepsilon}_f$, N and F are the free strain rate without substrate constraint, Poisson's ratio and uniaxial viscosity, respectively, of the wet coating. During drying, $\dot{\varepsilon}_f < 0$ and $\sigma_{con} \geq 0$. Therefore, the lateral constraint from the substrate results in a larger thickness shrinkage rate than the free shrinkage rate, i.e. $|\varepsilon_z| > |\varepsilon_f|$. With increase in pH value, the constraint on wet coating by substrate becomes weaker as the particles are more agglomerated. Therefore, less thickness shrinkage occurred with more agglomerated slurry (Table 1). On the other hand, the release of the constrained stress by crack formation decreased the thickness reduction rate, as measured in the later stage of the shrinkage (Fig. 5).

4.3. Cracking mechanism

Cracking behaviour of a wet coating depends on the balance between the coating shrinkage and substrate constrained stresses. The increase in agglomeration degree results in decrease in particle rearranging ability under capillary force, i.e. decrease in the relaxation ability of the tensile stresses applied by the substrate. Therefore, the agglomerated slurry tends to crack earlier compared to the dispersed slurry (Fig. 5 and Table 2).

Due to lateral flow, the densely packed region formed first at the coating edge, where the tensile stresses were higher than other positions. Therefore, cracks first formed at the coating edge and propagated towards the centre following the stress gradient. For the dispersed slurry with pH 3 (Fig. 5a), as cracks propagated, the crack width only increased slightly, indicating strong adhesion of the coating to the substrate. Tensile stresses were further built up, and new cracks formed and broke the previous fragments. When the drying entered into the FRP stage, less water was in the upper layer of the coating and more water in the bottom layer of the coating, resulting in a stress gradient across thickness. The fragments gradually folded up and detached from the substrate due to higher compressive force in the upper layer. Subsequently, spiral cracks were formed to relax the stress,[12] which also proved a strong adhesion of the coating to the substrate (Fig. 5a, images 6 and 7). For the strongly agglomerated slurry with pH 7.5, both the appearance of the annular gap (Fig. 5c, image 2) and rapid crack widening indicated weak adhesion between the coating and the substrate. The coating delaminated from the substrate quickly with increase in crack width. Therefore, the fragments could contract more freely and larger area surface contraction occurred with less number of cracks for the coatings cast from the agglomerated slurry. Moreover, the agglomerated slurry showed less effect of the final coating delamination on the drying rate with forming a less apparent 'hump' in Fig. 4a.

5. Conclusions

1. Irrespective of the agglomeration degree, the drying kinetics of the slurries cast on substrates was characterized as an initial CRP followed by a FRP. In the CRP stage, drying rate gradually decreased, followed by a sharp decrease in the FRP stage.
2. In the CRP stage, lateral drying led to uneven thickness reduction of the coating. With increase in agglomeration degree, the coating shrank more uniformly along surface. In addition, the coating shrank less along coating thickness, but contracted more along the surface.
3. Tensile stresses developed because of substrate constraint on the coating, and resulted in crack formation. The coating cast from more agglomerated slurry cracked earlier and showed weaker adhesion to the substrate.

Acknowledgement

Mel Chemicals is acknowledged for providing YSZ slurry.

References

1. Velamakanni, B. B. and Lang, F. F., Effect of interparticle potentials and sedimentation on particle packing density of bimodal particle size distributions during pressure filtration. *J. Am. Ceram. Soc.*, 1991, **74**, 166–172.
2. Lewis, J. A., Colloidal processing of ceramics. *J. Am. Ceram. Soc.*, 2000, **83**(10), 2341–2359.
3. Scherer, G. W., Theory of drying. *J. Am. Ceram. Soc.*, 1990, **73**(1), 3–14.
4. Smith, D. M., Scherer, S. W. and Anderson, J. M., Shrinkage during drying of silica gel. *J. Non-cryst. Solids*, 1995, **188**, 191–206.
5. Wang, X., Lan, W. H. and Xiao, P., Fabrication of yttria stabilized zirconia coatings by a novel slurry method. *Thin Solid Films*, 2006, **494**(1–2), 263–267.
6. Wang, Z. C., Shemilt, J. and Xiao, P., Fabrication of ceramic composite coatings using electrophoretic deposition, reaction bonding and low temperature sintering. *J. Eur. Ceram. Soc.*, 2002, **22**(2), 183–189.
7. Hu, M. S., Thouless, M. D. and Evans, A. G., Decohesion of thin films from brittle substrates. *Acta Metall.*, 1988, **36**(5), 1301–1307.
8. Chiu, R. C., Garino, T. J. and Cima, M. J., Drying of granular ceramic films. I. Effect of processing variables on cracking behaviour. *J. Am. Ceram. Soc.*, 1993, **76**(9), 2257–2264.
9. Chiu, R. C. and Cima, M. J., Drying of granular ceramic films. II. Drying stress and saturation uniformity. *J. Am. Ceram. Soc.*, 1993, **76**(11), 2769–2777.
10. Guo, J. J. and Lewis, J. A., Aggregation effects on the compressive flow properties and drying behaviour of colloidal silica suspension. *J. Am. Ceram. Soc.*, 1999, **83**(9), 2345–2358.
11. Shorlin, K., Debruyn, J., Graham, M. and Morris, S., Development and geometry of isotropic and directional shrinkage-crack patterns. *Phys. Rev. E*, 2000, **61**, 6950–6957.
12. Neda, Z., Leung, K., Jozsa, L. and Ravasz, M., Spiral cracks in drying precipitates. *Phys. Rev. Lett.*, 2002, **88**, 095502.
13. Lan, W.H. and Xiao, P., Constrained drying of aqueous Yttria-stabilised-zirconia slurry on a substrate. I. Drying mechanism. *J. Am. Ceram. Soc.*, 2006, in press.
14. Lgoh, G. K., Donthu, S. K. and Pallathadka, P. K., Cracking and orientation of solution-deposited rutile TiO_2 films. *Chem. Mater.*, 2004, **16**, 2857–2861.
15. Shibata, H., Study for the standardization of the drying curves of capillary-porous medias. *Ind. Eng. Chem. Res.*, 2005, **44**, 6865–6873.
16. Liu, H. K. and Parvizi-Majidi, A., Effect of particle additions on drying stresses and the green density of sol-gel-processed three-dimensional ceramic matrix somposites. *J. Am. Ceram. Soc.*, 1998, **81**(7), 1824–1828.
17. Deegan, R. D., Bakajin, O., Dupont, T. F., Huber, G., Nagel, S. R. and Witten, T. A., Capillary flow as the cause of ring stains from dried liquid drops. *Nature*, 1997, **389**, 827–830.
18. Hu, H. and Larson, G., Evaporation of a sessile droplet on a substrate. *J. Phys. Chem. B*, 2002, **106**, 1334–1344.
19. Martines, C. J. and Lewis, J. A., Shape evolution and stress development during latex-silica film formation. *Langmuir*, 2000, **18**, 4689–4698.
20. Routh, A. F. and Russel, W. B., Horizontal drying fronts during solvent evaporation from latex film. *AIChe J.*, 1998, **44**(9), 2088–2098.
21. Scherer, G. W., Drying gels. VIII. Revision and review. *J. Non-cryst. Sol.*, 1989, **109**, 171–182.